Organic Electronics 11 (2010) 207–211

Contents lists available at ScienceDirect

Organic Electronics

journal homepage: www.elsevier.com/locate/orgel

The role of the dielectric interface in organic transistors: A combined device and photoemission study

Philipp Stadler [a,*], Anna M. Track [b], Mujeeb Ullah [c], Helmut Sitter [c], Gebhard J. Matt [c], Georg Koller [b], Thokchom B. Singh [a], Helmut Neugebauer [a], N. Serdar Sariciftci [a], Michael G. Ramsey [b]

[a] Linz Institute for Organic Solar Cells (LIOS) and Institute for Physical Chemistry, Johannes Kepler University Linz, Altenbergerstr. 69, 4040 Linz, Austria
[b] Institute for Physics, University of Graz, Universitätsplatz 3, 8010 Graz, Austria
[c] Institute of Semiconductor and Solid State Physics, Johannes Kepler University Linz, Altenbergerstr. 69, 4040 Linz, Austria

ARTICLE INFO

Article history:
Received 17 August 2009
Received in revised form 19 October 2009
Accepted 23 October 2009
Available online 29 October 2009

Keywords:
Organic field effect transistor
Ultra-violet photoemission spectroscopy
Interface dipole
Energy level alignment
Threshold voltage shift

ABSTRACT

Here the device performance is shown to be directly related to the measured electronic level alignment at the dielectric interface in C_{60} organic field effect transistors (OFETs). We compare C_{60} on two dielectrics: Al_2O_3 and a divinyltetramethyldisiloxane-bis(benzocyclobutene) (BCB)–Al_2O_3 bilayer. The improved transistor performance and the lowering of the threshold voltage by 0.8 V due to the BCB interlayer are reflected in the ultra-violet photoemission data. These show a 0.8 eV difference in the work function and a concomitant shift in the C_{60} valence band. By following the work function the improvement is shown to be due to the dipole at the organic BCB–C_{60} interface.

1. Introduction

Interface engineering in organic field effect transistors (OFETs) has become the key issue in designing devices with acceptable electrical transport properties. The crucial part is to design the interface between the dielectric and the organic semiconductor [1]. It has been demonstrated that by introducing a polymeric layer on an oxidic dielectric surface the overall device performance can be enhanced. Recent publications demonstrate well performing transistors with passivation layers of various thin polymeric insulators as well as transistors with self assembled molecules (SAMs) grown on silicon dioxide and Al_2O_3 [2–6]. Factors ranging from film morphology through to issues of electronic level alignment could all be playing a role. While device activity has concentrated on modifying the inorganic dielectric surface with SAMs or polymer dielectrics, little work has considered the possibility of charge rearrangements at the interface of such modifiers with the organic semiconductor. Recently theoretical modelling has suggested that improvements in transfer characteristics and rigid shifts of the threshold voltage can result from the introduction of permanent space charge or dipole layers at the organic semiconductor/dielectric interface [7]. In particular the introduction of a BCB divinyltetramethyldisiloxane-bis(benzocyclobutene) interlayer between the inorganic dielectric (Al_2O_3, SiO_2) and the organic semiconductor has been reported to yield low operating voltages and high mobilities [2–4]. Apart from suggestions of it acting as a passivation layer removing hydroxyl groups from the semiconductor dielectric interface little is known of the function of BCB interlayers. Till now very few combined studies of device characteristic and photoemission investigations of the energy level alignment of device structures can be found in literature [8]. Moreover, to our knowledge there have been no such studies where a

* Corresponding author. Tel.: +43 732 2468 8854; fax: +43 732 2468 8770.
E-mail address: Philipp.Stadler@jku.at (P. Stadler).

1566-1199/$ - see front matter © 2009 Elsevier B.V. All rights reserved.
doi:10.1016/j.orgel.2009.10.017

comparison of device structures with and without interlayer has been made.

In this work transistors using C_{60} and a bilayer of BCB–Al_2O_3, which has been reported to have low operation voltage (~1 V) and high mobilities (<3 $cm^2 V^{-1} s^{-1}$) [2,3], were used to explore the role in the improved performance due to the BCB interlayer. Here a systematic study of two insulator-C_{60} structures, with and without BCB, is made. We compare the performance of the field effect transistors and show that the improvement of the OFET with BCB can be directly related to the differences in energy level alignment as measured by ultra-violet photoemission spectroscopy (UPS). Moreover, from studies of each interface the improvement in device performance arising from the polymeric interlayer is shown to be generated by an in-built potential at the BCB-interlayer/organic semiconductor interface.

2. Experimental section

Here we use the same OFET system as Zhang et al. [3] and we systematically compare the interface of C_{60} and BCB–Al_2O_3 to the interface of C_{60} and Al_2O_3 alone to understand its role in the improved performance. To allow meaningful comparison we fabricated two bottom-gate/top contact transistors, such that both the Al_2O_3 alone and the bilayer Al_2O_3–BCB exhibit the same geometric capacitance, as depicted in Fig. 1. Additionally using 55 nF cm^{-2} dielectric layers provide transistors operating at gate voltages in the range of 1 V and a mobility of 1 $cm^2 V^{-1} s^{-1}$. To combine the transistor with the photoemission spectroscopy the same MIS structures are studied by UPS with the samples prepared in a controlled way using the same batch at once and a blind sample as a reference for the surface characterization.

2.1. OFET fabrication and characterization

BCB precursor solution and C_{60} was purchased from Aldrich and Merck respectively. The C_{60} was purified in a further re-sublimation process before evaporation. 200 nm of Al are deposited on a glass substrate at a rate of 10 Å s^{-1}. For the Al_2O_3 gate insulator a 145 nm and an 85 nm film respectively is electrochemically grown on the Al following the instructions from Majevski et al. [9] and Schröder et al. [10]. The generated oxide was then rinsed and treated with distilled water at 80 °C in the ultra sonic bath and finally dried at 200 °C. For the polymer layer a 1 wt% BCB precursor solution in mesitylene was spun onto the 85 nm thick aluminium oxide film at 1500 rpm and afterwards annealed at 150 °C for cross linking. By controlling the Al_2O_3 thickness we obtained two systems (Al_2O_3 layer and Al_2O_3–BCB bilayer) with similar surface roughness of 1.5 nm RMS and with the same measured geometric capacitance C_p of 55 nF cm^{-2}. The thicknesses were measured by capacitance measurements (Al–Al_2O_3–Al) and checked by cross section scanning electron microscopy. For the semiconductor a 300 nm C_{60} film was deposited in high vacuum using hot wall epitaxy technique at a substrate temperature of 140 °C and a growth rate of 0.5 Å s^{-1} [11]. The morphologies, as determined by AFM of the C_{60} films on the two substrates are found to be similar. For the source-drain contacts LiF/aluminium (0.6 and 50 nm) [12] was evaporated using a 70 μm shadow mask for the channel and a channel width W of 2 mm. The OFETs were characterized using Agilent E5273A 2-channel-source unit.

2.2. UPS measurements at dielectric-semiconductor interface

For the UV photoemission spectroscopy metal–insulator–semiconductor structures were prepared in the following way: A 5 nm thin layer of aluminium oxide was electrochemically grown on aluminium and treated afterwards as mentioned in Section 2.1. For the BCB surface, the 1% precursor solution was directly spun onto oxidized aluminium and cured at 200 °C as for the transistor. In a further step the C_{60} was deposited by thermal evaporation at a rate of 1 A s^{-1} at a substrate temperature of 78 K in order to guarantee homogenous covering. The thickness of the C_{60} is 2 nm (3–4 molecule layers) as determined by a quartz microbalance calibrated for C_{60}. The samples were then characterized by HeI (21.2 eV) UPS in ultra high vac-

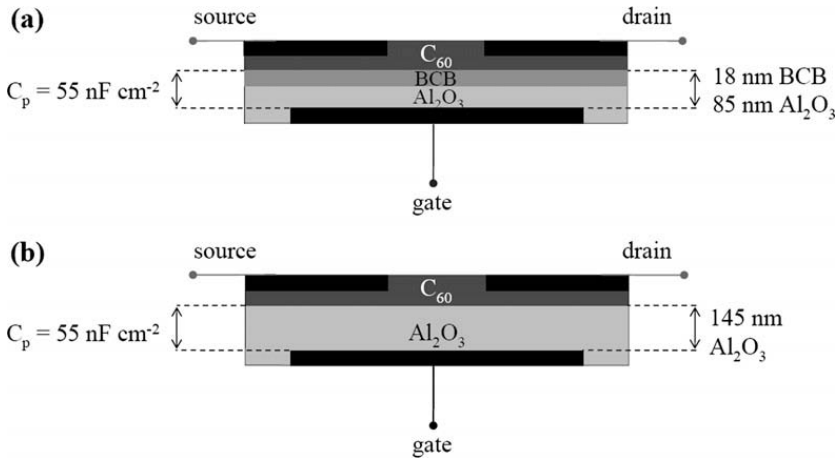

Fig. 1. Schematic of the OFET structures studied with (a) and without (b) a BCB layer on Al_2O_3. Both structures exhibit the same geometric capacitance of 55 nF cm^{-2}.

uum using a Specs PHIOBOS hemispherical energy analyser. The valence band spectra were recorded in both normal and 45° off normal emission angles and the work functions were determined from the secondary electron cut off in normal emission with a bias of 10 V. For all films XPS spectra were taken and no significant contamination was observed.

3. Results and discussion

3.1. OFET characterization

The device characteristic with and without BCB are compared in Fig. 2a and b which show the output characteristics and the transfer characteristics taken in the linear regime ($U_{gate} > U_{drain}$), respectively. Data presented here are recorded when the gate voltage U_{gate} as well as the drain voltage U_{drain} are applied in ascending and descending mode with 1 s integration time per step. Both figures reflect the same trend, however, the transistor with the BCB interlayer performs significantly better in all respects. It has a higher source-drain current I_{ds}, a higher depletion and accumulation amplitude, a sharper onset, a higher on/off ratio and a lower hysteresis. The observed hysteresis in the transfer curve is reduced for the BCB–C_{60} and the charge charier mobility μ in the range of 1 $cm^2 V^{-1} s^{-1}$ is in good agreement to earlier results of C_{60} on BCB [2,13,14].

The most striking difference of the two systems is the tremendous change in the threshold voltage U_{th}: To extract the exact threshold value in the linear regime, the transconductance change or second derivative (SD) method is selected [15]. The method estimates U_{th} as the gate voltage at which the derivative of the transconductance (dI/dU_{gate}) is maximum [16]. It works around the problem of series resistances and is shown to give reliable values for organic (n-channel) systems [17]. In Fig. 3a, the second derivative of the transfer characteristics d^2I/dU^2_{gate} is presented showing two maxima. The device with BCB shows a distinct and sharp peak, whereas for the device without BCB the peak is rather broad and ill-defined.

The peak maximum corresponds to the threshold voltage U_{th} of the transistor system which shifted from +725 mV in the Al_2O_3–C_{60} interface system to −75 mV in the BCB–C_{60} interface system. The device with the BCB interlayer has a 0.8 V lower U_{th}.

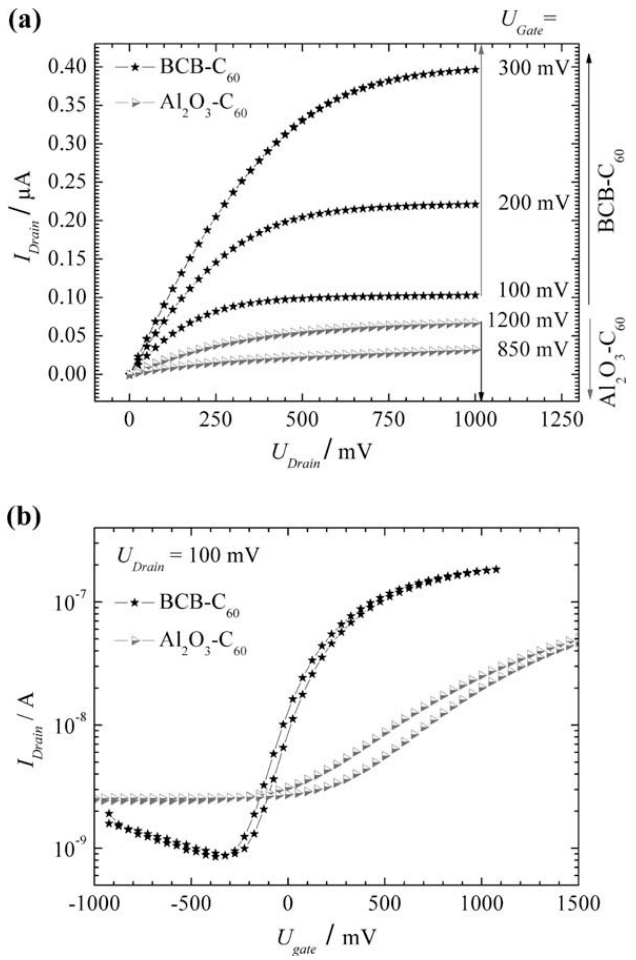

Fig. 2. Output characteristics (a) and transfer characteristics (b) in the linear regime ($U_{drain} < U_{gate} - U_{th}$) of both OFETs with (dark) and without (light) BCB layer on Al_2O_3.

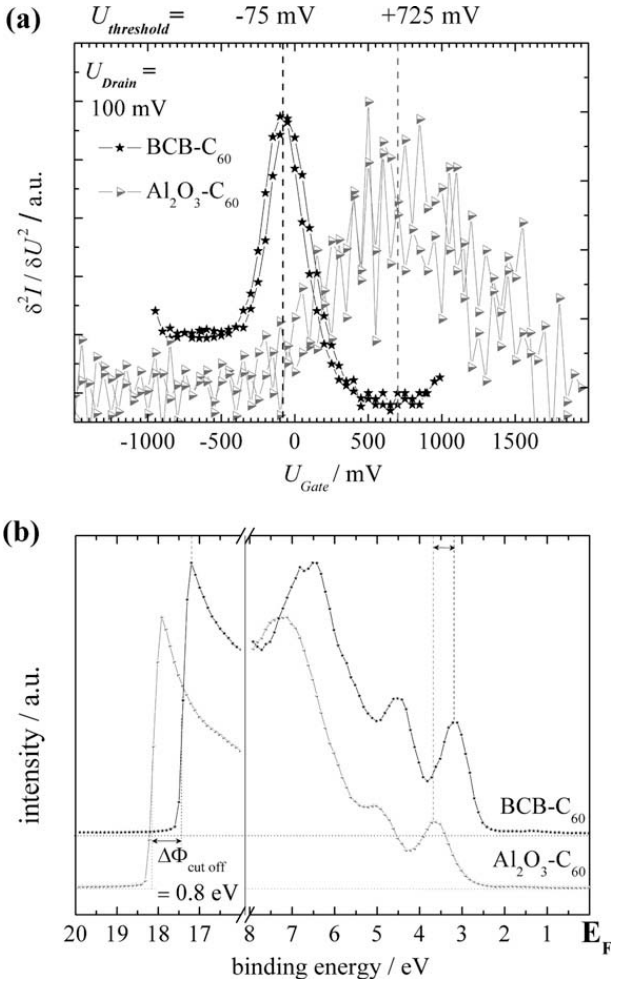

Fig. 3. (a) Shift of threshold voltage ΔU_{th} as seen in the second derivative of the transfer characteristics in OFETs with (dark) and without (light) BCB layer. (b) The UV photoemission spectrum of C_{60} on Al_2O_3 (light) and on BCB (dark) referenced to the Fermi energy. The shift in the HOMO and in the secondary electron cut-off $\Delta\Phi$ is indicated.

3.2. Photoemission studies

Photoemission measurements of ex situ prepared films on dielectric substrates are particularly challenging as contamination and charging effects can be misleading and care has to be taken. In Fig. 3b the UPS spectra of $Al/Al_2O_3/BCB/C_{60}$ and $Al/Al_2O_3/C_{60}$ thin film structures are shown referenced to the Fermi energy obtained from a metal substrate. In both cases the valence band fingerprint of the uppermost C_{60} layer is well defined with a quality approaching that of in situ UHV prepared C_{60} films [18]. This, combined with the fact that the ionisation potential of C_{60} in both cases are in agreement with literature values [18], shows that contamination and charging effects are minor.

The comparison of Fig. 3a and b illustrates the link between the device thresholds U_{th} and the electronic level alignment observed in the UPS spectra with BCB and without BCB. Clearly, introducing the BCB interlayer leads to a rigid shift of the entire photo emission spectrum to lower binding energy relative to the Fermi level. The shift of the HOMO-peak is measured to be 0.6 eV whereas the shift in the secondary cut-off, the change in the work function, is 0.8 eV. Thus the change in the measured C_{60} electronic level alignment induced by the BCB layer is the same as the lowered threshold voltage measured in the device with BCB.

To determine where and why the BCB has lowered the threshold voltage UPS spectra were measured at each layer in the device. This is summarized in Fig. 4 where the energy relations of the studied metal–insulator–semiconductor (MIS) systems for all interfaces with the work function measured for each layer are indicated. For the pure inorganic dielectric device without BCB (Fig. 4a) we measured a large work function drop to 2.7 eV on oxidation of the aluminium surface followed by a very small increase of the work function to 2.9 eV when the C_{60} film is grown on the oxide. Similar changes have been observed in in situ model studies [19,20]. In contrast, what is seen in Fig. 4b, is that on applying BCB to the Al_2O_3 surface the work function drops further to 2 eV. Then when C_{60} is grown on the BCB surface there is a large increase of the work function to 3.7 eV. At both BCB interfaces (Al_2O_3 and C_{60}) significant dipoles are formed and clearly BCB cannot be considered simply a passive spacer layer. The large work function increase at the BCB–C_{60} interface is the prime determinant of the improved device performance.

The result suggests that a significant interface dipole is formed at the BCB–C_{60} interface. This is surprising as generally organic–organic interfaces display vacuum level alignment with no significant interface dipoles. However in recent model studies [21] significant interface dipoles at organic–organic interfaces have been observed and were attributed to integer charge transfer (ICT) that is the formation of polaronic charge transfer states. Indeed the observed work function increase for C_{60} on P3HT has been attributed to this effect [21].

The C_{60} level alignments on the two gate dielectrics measured in the UPS are consistent with the two threshold voltages measured for the OFETs. Gate voltages of −0.075 V (BCB–C_{60}) and +0.725 V (Al_2O_3–C_{60}), would shift the HOMO level in both cases to around 2.8 eV below the Fermi level of the source. As C_{60} is a *n*-type semiconductor it is the LUMO relative to the Fermi energy of the source that is critical. Given a C_{60} affinity level of ~2.5 eV above the HOMO [21,22] one sees that the device threshold is obtained when the electron affinity is positioned slightly below the Fermi level of the source.

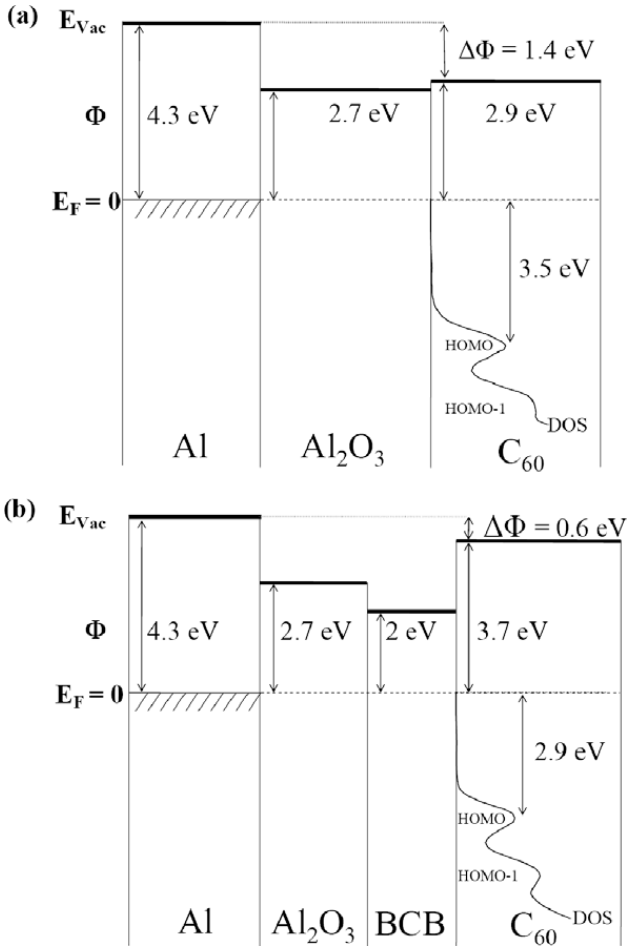

Fig. 4. Measured energy level diagrams of the two metal–insulator–semiconductor (MIS) structures studied without (a) and with (b) BCB between C_{60} and Al_2O_3. The Fermi level is the reference level and the work function at each layer are indicated. Note the large work function change at the BCB–C_{60} interface (b) and that the difference in the final work function between the two structures is 0.8 eV.

4. Conclusion

To conclude we studied two different interfaces between an organic semiconductor (C_{60}) and oxide (Al_2O_3) and an organic polymer (BCB) respectively. At the BCB interlayer dipoles are formed, which lower the threshold voltage and improve the transistor performance. The 0.8 V difference in the threshold voltage of the two device structures has been shown to be directly related to the 0.8 eV work function differences and is consistent with the band offset of C_{60} in each device. Photoemission investigations at all interfaces clearly indicate that the dipole formed at the BCB–C_{60} interface is the prime determinant for the improved device threshold. The magnitude and mechanism of this shift suggests detailed studies into tailoring

organic–organic interfaces on the gate dielectric could be very promising for optimizing device performance.

Acknowledgments

Work at Johannes Kepler University Linz and University of Graz was performed within the Nationales Forschungs Netzwerk (NFN) "Interface controlled and functionalised organic thin films" from the Austrian Foundation for Advancement of Scientific Research (FWF P15629).

References

[1] M. Mottaghia, G. Horowitz, Org. Electron. 7 (2006) 528–536.
[2] X.-H. Zhang, B. Kippelen, Appl. Phys. Lett. 93 (2008) 133305.
[3] X.-H. Zhang, B. Domercq, B. Kippelen, Appl. Phys. Lett. 91 (2007) 092114.
[4] L.-L. Chua, J. Zaumseil, J.-F. Chang, E.C.-W. Ou, P.K.-H. Ho, H. Sirringhaus, R.H. Friend, Nature 434 (2005) 195.
[5] C. Celle, C. Suspène, J.-P. Simonato, S. Lenfant, M. Ternisien, D. Vuillaume, Org. Electron. 10 (2009) 119–126.
[6] H. Klauk, U. Zschieschang, M. Halik, J. Appl. Phys. 102 (2007) 074514.
[7] S. Possanner, K. Zojer, P. Pacher, E. Zojer, F. Schürrer, Adv. Funct. Mater. 19 (2009) 958–967.
[8] Yunseok Jang, Jeong Ho Cho, Do H. Kim, Y.D. Park, M. Hwang, K. Cho, Appl. Phys. Lett. 90 (2007) 132104.
[9] L.A. Majewski, R. Schroeder, M. Grell, P.A. Glarvey, M.L. Turner, J. Phys. D: Appl. Phys. 37 (2004).
[10] R. Schroeder, L.A. Majewski, M. Grell, Adv. Mater. 16 (2004) 633.
[11] A. Andreev, C. Teichert, G. Hlawacek, H. Hoppe, R. Resel, D.-M. Smilgies, H. Sitter, N.S. Sariciftci, Org. Electron. 5 (2004) 23–27.
[12] C. Brabec, S. Shaheen, C. Winder, P. Denk, N.S. Sariciftci, Appl. Phys. Let. 80 (2002) 1288–1290.
[13] T. Anthopoulos, T.B. Singh, N. Marjanovic, N.S. Sariciftci, A. Ramil, H. Sitter, M. Cölle, D. de Leeuw, Appl. Phys. Lett. 89 (2006) 213504-1.
[14] T.B. Singh, N.S. Sariciftci, Annual Review of Material Research 36 (2006) 199–230.
[15] G. Horowitz, Adv. Mater. 10 (1998) 365–377.
[16] H.-S. Wong, M.H. White, T.J. Krutsick, R.V. Booth, Solid-State Electron. 30 (1987) 953.
[17] D. Boudinet, G.L. Blevennec, C. Serbutoviez, J.M. Verilhac, H. Yan, G. Horowitz, J. Appl. Phys. 105 (2009) 084510.
[18] S.J. Kang, Y. Yi, C.Y. Kim, S.W. Cho, M. Noh, K. Jeong, C.N. Whang, Syn. Met. 156 (2006) 32–37.
[19] J. Ivanco, B. Winter, L. Gregoratti, M. Kiskinova, F.P. Netzer, M.G. Ramsey, Appl. Phys. Lett. 85 (2004) 585–587.
[20] R.I.R. Blyth, S.A. Sardar, F.P. Netzer, M.G. Ramsey, Appl. Phys. Lett. 77 (2000) 1212–1214.
[21] W. Osikowicz, M.P. de Jong, W.R. Salaneck, Adv. Mater. 19 (2007) 4213–4217.
[22] I.F. Torrente, K.J. Franke, J.I. Pascual, J. Phys.: Condens. Matter 20 (2008) 184001.